Published in "Journal of Physics and Chemistry of Solids
doi:10.1016/j.jpcs.2011.02.009 , 2011"
which should be cited to refer to this work.

High temperature magnetic order in zinc sulfide doped with copper

Frank J. Owens [a,b], L. Gladczuk [c,*], R. Szymczak [c], P. Dluzewski [c], A. Wisniewski [c], H. Szymczak [c], A. Golnik [d], Ch. Bernhard [e], Ch. Niedermayer [f]

[a] Army Armament Research, Development and Engineering Center, Picatinny, NJ 07806, USA
[b] Department of Physics, Hunter College, City University of New York, NY 10024, USA
[c] Institute of Physics, Polish Academy of Sciences, Aleja Lotnikow 32/46, PL-02-668 Warsaw, Poland
[d] Institute of Experimental Physics, University of Warsaw, Hoza 69, PL-00-681 Warsaw, Poland
[e] Department of Physics and FriMat Center for Nanomaterials, University of Fribourg, Chemin du Musee 3, CH-1700 Fribourg, Switzerland
[f] Laboratory for Neutron Scattering, ETH Zurich and Paul Scherrer Institute, CH-5232 Villigen PSI, Switzerland

We report the first observation of magnetic order above room temperature in zinc sulfide doped with Cu^{2+} made by a simple sintering process and detected by ferromagnetic resonance (FMR), SQUID magnetometry and the μSR experiments. FMR study shows nonzero absorption above room temperature indicating a high value of Curie temperature. Field-cooled and zero-field-cooled magnetization data indicate a bifurcation at about 300 K. This temperature is considered to be the blocking temperature at ferromagnetic nanosized regions, which appear to exist in the sample of ZnS doped with copper. The muon spin rotation measurements confirm highly nonuniform magnetic order. It was shown that about 25% of the sample volume fraction exhibits strong magnetism.

1. Introduction

In recent years there is much research aimed at developing dilute magnetic semiconductors, (DMS), having Curie temperature above room temperature. DMS are considered as ideal materials for spintronic devices. Storage of information currently employs magnetic field alignment of rod like ferromagnetic nanoparticles. Switching uses separate metal oxide semiconducting field effect transistors in which the flow of current is controlled by a voltage on the gate. The effort to develop DMS materials involves synthesizing alloys of semiconducting materials and magnetic ions such as Mn^{2+} or Cu^{2+} typically by ion implantation or molecular beam epitaxy methods [1–4]. There also have been some reports of fabrication of DMS materials with Curie temperature well above room temperature by solid state sintering techniques, which should be less expensive in large scale production [5,6]. Dietl et al. [7] have proposed that the ferromagnetism results from a mediation of the exchange interaction by holes or electrons between the paramagnetic dopants. In the ferromagnetic state there is a splitting of the valence and conducting band depending on the spin orientation of the charge carriers. The model predicts that hole doped semiconductors will have higher Curie temperature than electron doped materials. Another important question, as discussed by Dietl [8,9], is whether a spatially uniform ferromagnetic spin order is a real ground state of all semiconductors doped with magnetic ions. He argues that very often in these materials nano-scale phase separation into regions with a large and small concentration of the magnetic component takes place. High-temperature ferromagnetism has been observed in semiconductors doped with copper ions such as Cu doped GaP made by a solid state sintering process [6]. Copper is a better dopant choice than manganese because unlike manganese nanoparticles, copper nanoparticles are not known to be ferromagnetic and their precipitation in forms of clusters does not contribute to ferromagnetism since such dopant is naturally and intrinsically nonmagnetic. Moreover the calculations using the plan-wave pseudopotential method indicate the ferromagnetic ordering and spin-resolved electronic properties of in Cu-doped ZnS [10,11].

However, there have been some sintering synthesis reported that produced no ferromagnetism [12]. This is likely due to differences in fabrication conditions. It is known that the ability to produce the ferromagnetic phase by sintering is quite sensitive to conditions requiring a relatively low temperature of the order of 500 °C. Synthesis at higher temperatures generally does not produce a ferromagnetic phase. However, the observation of ferromagnetism in Mn doped ZnO has been detected by different methods such as magnetic circular dichroism and Faraday rotation [13]. In this work, we present ferromagnetic resonance, SQUID magnetometry and muon spin relaxation evidence for

* Corresponding author.
E-mail address: gladl@ifpan.edu.pl (L. Gladczuk).

the existence of ferromagnetism in ZnS doped with copper and synthesized by a solid state sintering process. These studies were stimulated by information on preparation of homogeneous highly doped ZnS:Cu nanoparticles [14]. Zinc sulfide is an important II–VI compound having potential applications in electronics and optoelectronics because of its wide band gap of 3.72 eV. The existence of a DMS in ZnS should have interesting spintronic applications.

2. Experimental

The samples were synthesized by thoroughly mixing in the ratio 0.04 molecular weight of CuS to one molecular weight of ZnS and then grinding the mixture using a mortar and pestle. The samples in the form of pressed pellets contained in an alumina boat were sintered at 500 °C in an oven for four hours in air followed by rapid quenching to room temperature. Measurements of the magnetic properties were made using SQUID magnetometry, ferromagnetic resonance (FMR) and muon spin rotation (μSR). The FMR measurements were made using a Varian E-9 spectrometer operating at 9.2 GHz with 100 KHz. modulation. The temperature of the sample was controlled by flowing heated or cold nitrogen gas through a double-walled quartz tube, which is a part of an ADP Heli–Tran system, and which is inserted through the center of the microwave cavity. The sample was contained in the quartz tube and located at the center of the cavity. The magnetization was measured using a Quantum Design MPMS5 SQUID magnetometer. The measured magnetization was corrected for the diamagnetic contribution due to pure ZnS. Raman measurements were made using a J.Y. Horiba confocal micro-Raman system employing a 25 mW He–Ne laser focused to a spot having a 15 micron radius and having a wavelength of 632.8 nm. X-ray diffraction patterns were measured using a X'Pert powder diffractometer ($Cu_{K\alpha}$ radiation). The sintered samples were examined by Induction Coil Plasma mass spectrometry (ICP-MS), which showed no magnetic metals at levels that could account for the observed ferromagnetism. The presence of copper in the samples was however detected. Probably this is associated with unreacted CuS which, as discussed below, is observed in resonance measurements.

The starting ZnS material was examined by electron paramagnetic resonance prior to processing and no evidence of any paramagnetic or ferromagnetic material was detected. Paramagnetic resonance is sensitive to such species to one part in 10 billion.

In order to determine the volume fraction of the magnetic phase in the samples, the muon spin rotation experiments were performed at the piM3 muon beamline with the GPS (general purpose setup) at the Paul-Scherrer Institute in Villigen, Switzerland.

3. Results and discussion

Fig. 1 shows the powder X-ray diffraction pattern of Cu doped ZnS. The peaks in the doped sample occur at the same scattering angles as in pure ZnS suggesting that Cu^{2+} substitutes for zinc in the lattice. Since Cu^{2+} and Zn^{2+} have very similar ionic radii (0.71 and 0.74 Å, respectively) no expansion or contraction of the lattice parameters that could cause shifts in the diffraction peaks would be expected. A change in lattice parameters would be expected if the Cu is at interstitial sites. There is some evidence in the XRD for small amount of ZnO in the sample which is not unexpected because the sintering was done in air. Due to excellent statistics of the applied counter, an unidentified phase(s) of insignificant quantity (peaks at 21.2°, 26.9° and 35.0° 2θ of intensity $< 2\%$) was detected. The diffraction pattern presented in Fig. 1 differs from

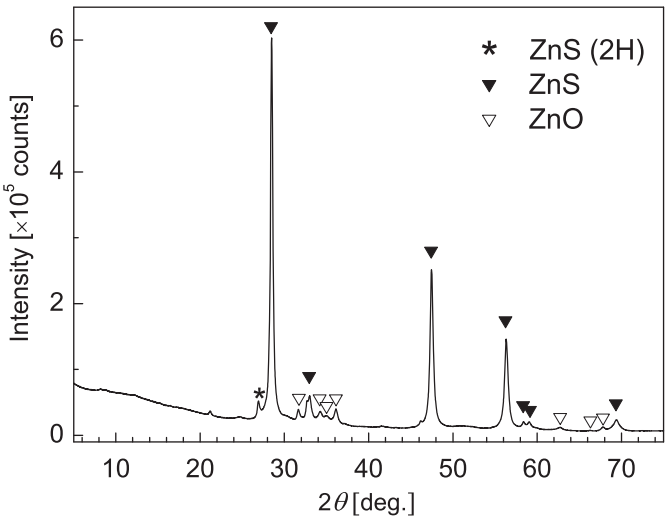

Fig. 1. X-ray diffraction of ZnS:Cu.

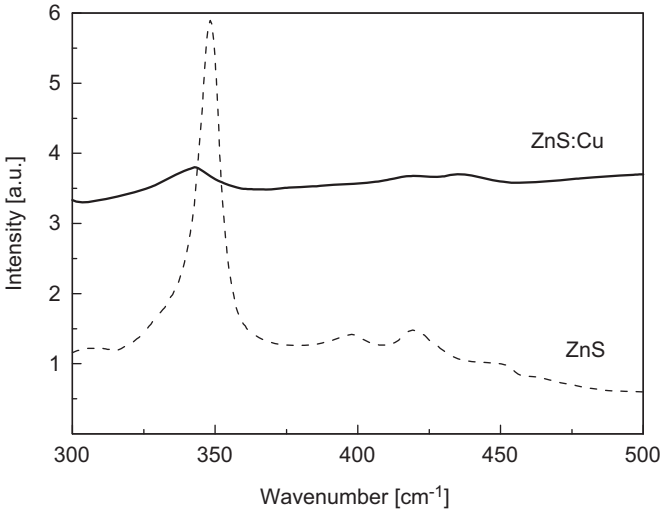

Fig. 2. Raman spectra in doped (top) and undoped (dashed line) ZnS showing reduction in frequency of LO mode in doped sample.

that for ZnS:Cu nanoparticles [14] by individual peak width, due to the difference in crystallite size.

The Raman spectrum of undoped zinc sulfide consists of two strong lines at 261 and 348 cm^{-1}, which have been assigned in previous work to the transverse optical (TO) and longitudinal optical (LO) modes, respectively [15]. The smaller peaks above 350 cm^{-1} have been identified as second order modes [16]. The Cu doped sample shows stronger photoluminescence than the undoped one when subjected to the laser light and it is not possible to observe the TO mode. However, it is possible to detect the LO mode which has shifted down to 339 cm^{-1} as shown in the top of Fig. 2. The lower spectrum in Fig. 2 (dashed line) is of the ZnS material. It is unlikely that this down shift is a consequence of an expansion of the lattice parameters on doping since the XRD results does not indicate such an expansion. A possible explanation involves a coupling of the plasma mode to the LO mode. It has been shown that when GaP is doped with Cu^{2+} or Mn^{2+}, which results in hole doping of the material, the LO mode shifts to lower frequency [6,17]. This is because the LO mode is coupled to the plasma mode whose frequency depends on the electron concentration. Hole doping decreases the electron concentration and therefore the plasma frequency. However, Cu^{2+}

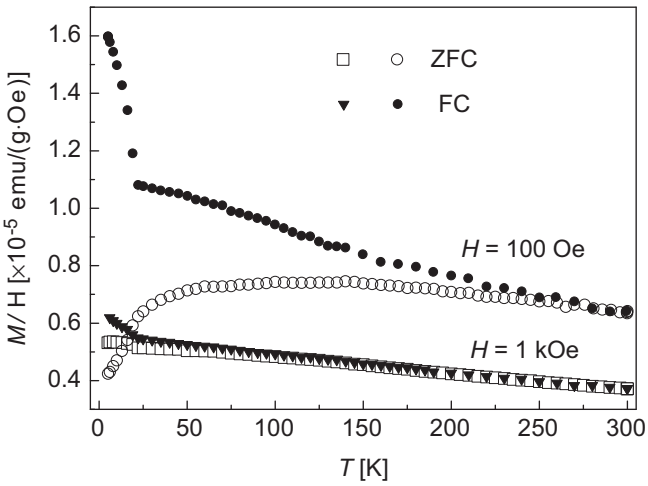

Fig. 3. The susceptibility measured in magnetic fields 100 Oe and 1 kOe as a function of temperature. Both zero-field-cooled (ZFC) and field-cooled (FC) curves are shown.

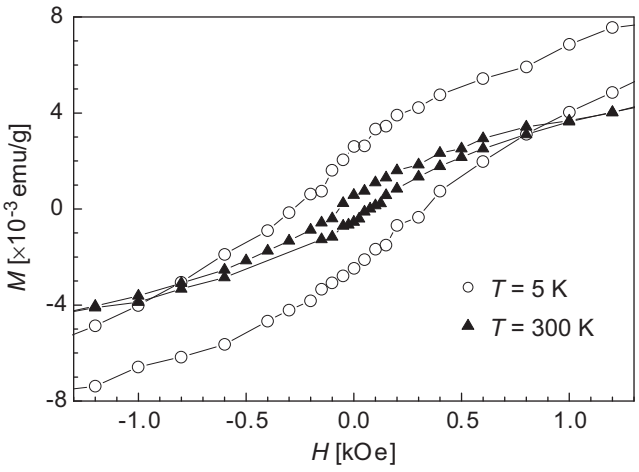

Fig. 4. Hysteresis loops measured at temperatures 5 and 300 K.

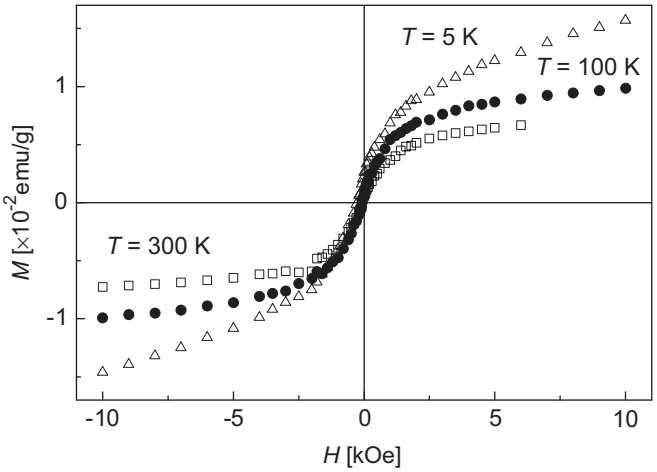

Fig. 5. Magnetization curves measured at temperatures 5, 100 and 300 K.

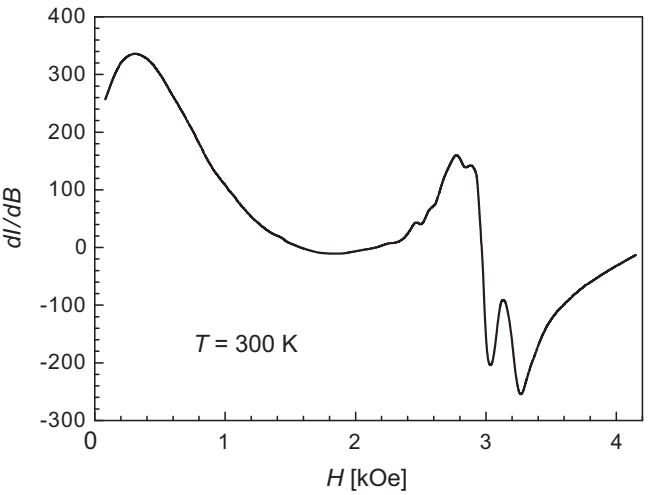

Fig. 6. Ferromagnetic resonance spectrum, derivative of the absorption I with respect to B, recorded at room temperature.

doping of ZnS should not produce holes. The hole doping may occur during the high temperature processing which may increase the number of defects.

Fig. 3 displays the temperature dependence of the susceptibility in zero-field-cooled (ZFC) and field-cooled (FC) samples measured by the SQUID magnetometer. Measurements were taken in applied fields of 100 Oe and 1 kOe. The splitting between the FC and ZFC curves is characteristic of dynamical behavior of magnetic nanoparticles indicating the presence of a blocking temperature near room temperature. This suggests that the ferromagnetism occurs in nanosized ZnS:Cu regions as proposed by Dietl [8,9,18]. The observed difference between M_{FC} and M_{ZFC} is a direct measure of irreversibility in magnetization. In conventional ferromagnets, irreversibility in the magnetization is attributed to the domain structure. The bifurcation between the ZFC and the FC is also observed in superparamagnetic isolated nanoparticles. The striking features observed below ~25 K suggest presence of two contributions to irreversibility in magnetization having different dependences on temperature. The first contribution arises from the regions of the sample with long-range order and consequently with magnetic domains. The nanoparticles isolated from these ferromagnetic regions are responsible for second contribution to the irreversibility in the magnetization. This observation demonstrates that the systems investigated here is not a pure ferromagnetic but a mixed state in which long range ferromagnetic order coexists with superparamagnetic isolated nanoparticles. The magnetic hysteresis loops displaying small hysteresis measured at 5 and 300 K are shown in Fig. 4. The coercive field at temperature 5 K is 300 Oe and decreases to 75 Oe at 300 K. Fig. 5 shows the magnetic field dependence of the magnetization at 5, 100 and 300 K. The soft magnetic character is typical for dilute magnetic ferromagnetic materials that have low coercivity and low remanence. Note that at lower temperature the magnetization in the saturation region increases linearly with magnetic field strength and the slope of the dependence increases with lowering temperature. This likely is a result of the presence of unreacted CuS in the sample as indicated by the ICP-MS and the FMR data that will be discussed below.

Fig. 6 shows the FMR spectrum at 300 K recorded using a Varian E-9 spectrometer operating at 9.2 GHz. Three lines are evident in the spectrum, a low field non-resonant signal, a broad ferromagnetic resonance signal near 3 kOe and a narrower line superimposed on the broad FMR line which is likely due to some unreacted CuS in the sample. In a single crystal the magnetic field position of the FMR signal depends on the orientation of the dc magnetic field with respect to important symmetry directions in the unit cell. The spectrum shown here is from a collection of

randomly oriented grains and is powder pattern representing the weighted sum of spectra from all orientations of the dc magnetic field. It should be noted that CuS is not ferromagnetic and cannot be the source of the ferromagnetism observed here.

The low field non-resonant absorption signal has been observed in a wide variety of materials: high-temperature superconductors, ferrites, semiconductors and manganites [19–22]. The presence of this microwave absorption may be considered as an indication of ferromagnetism in materials [19,20]. The signal occurs because the permeability in the ferromagnetic state depends on the applied magnetic field, increasing at low fields to a maximum and then decreasing. Since the surface resistance depends on the square root of the permeability, the microwave absorption depends non-linearly on the strength of the dc magnetic field resulting in a non-resonant derivative signal centered at zero field. This signal is absent in the paramagnetic state and emerges as the temperature is lowered below Curie temperature T_C. Fig. 7 shows the temperature dependence of the magnetic field position and of the linewidth of the high field FMR signal above room temperature. The broadening and shift to lower magnetic fields of the FMR spectra with the decrease of temperature is typical of FMR spectra and provide further evidence for the existence of ferromagnetism above room temperature in copper doped ZnS.

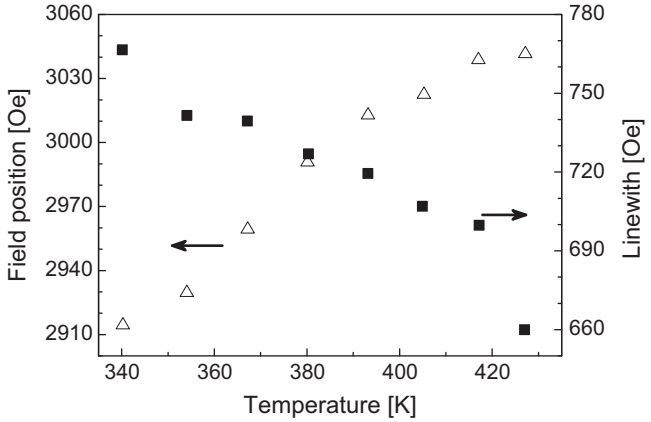

Fig. 7. Temperature dependence of field position (open circle) and of the linewidth (squares) of ferromagnetic resonance above room temperature.

The muon spin rotation (μSR) experiment, where implanted muons are used as a local probe of magnetic field distribution sensitive to short-range magnetism, was expected to provide complementary information on magnetism of the studied system. The weak transverse field configuration (wTF-μSR) was chosen for the present experiments. The 63 mg of ZnS:Cu crystallites was mounted on a thin mylar foil in order to cover a maximum area of the muon beam. Spin polarized positive muons are implanted into the samples with an energy of 4 MeV and come to rest without losing their spin polarization. The muon beam intensity is adjusted so that only one muon is present in the sample at a given time. The special veto electronic was used to reject the cases, when muon missed the sample and stopped elsewhere. In the TF-μSR experiments the external field is perpendicular to the spin polarization of the muon beam, thus the spin of the implanted μ^+ precesses around the field direction. The μ^+-spin precession frequency ω is given by the muon gyromagnetic ratio $\gamma_\mu/2\pi = 135.534\ \mathrm{MHz}/T$ and the value of the internal magnetic field at the muon site B, $\omega = (\gamma_\mu/2\pi)B$. The positive muon decays with a time constant of $\tau_\mu = 2.1971\ \mu\mathrm{s}$ into the positron and two neutrinos. Since the positron is emitted preferentially in the direction of muon spin, the spin precession can be registered by detecting the positrons emitted at given direction as a function of time between the muon implantation and its decay. Four positron counter were placed at the angles θ_i to the initial direction of the muon spin, so the obtained histogram for each counter obeys the relation

$$N_i(t) = N_{0i}(t)[1 + A_i G_x(t)\cos(\omega t + \theta_i)]\exp(-t/\tau_\mu) + B_{0i} \quad (1)$$

where B_{0i}, N_{0i} and A_i are the background, normalization and asymmetry constants, respectively, for each counter. $G_x(t)$ is called depolarization function describing the line broadening due to a spread of internal fields (dephasing) and muon spin relaxation.

The theory of weak interaction predicts the value of 1/3 for the muon decay asymmetry A, but the observed value of A is usually lower, mainly because of the finite solid angle covered by the positron counter. The actual values of A_i for each counter were determined in previous experiments on the same setup with

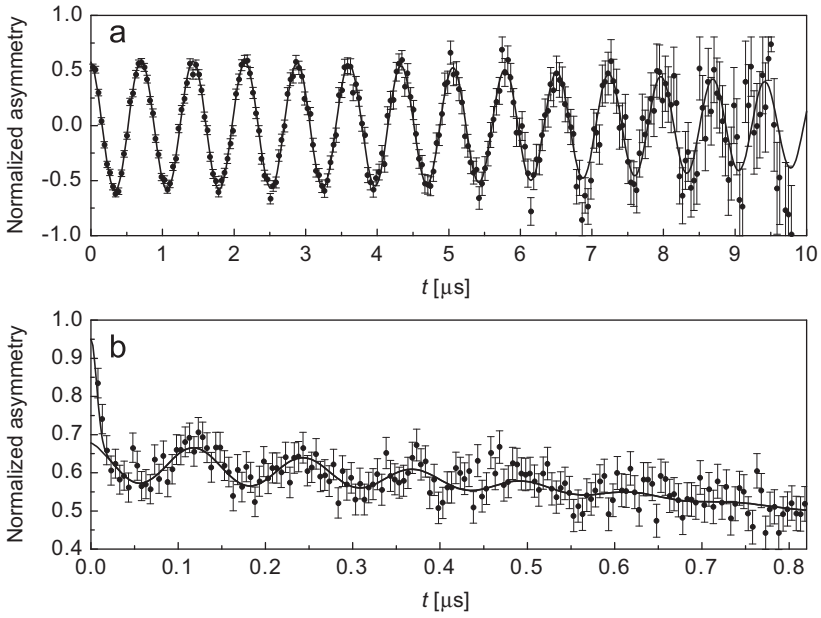

Fig. 8. The normalized muon asymmetry spectra for $T = 150$ K and two values of external magnetic field (a) 100 Oe and (b) 5.3 Oe.

nonmagnetic samples. Hence we were able to determine the absolute fractions of muons stopped in ZnS:Cu samples experiencing different internal magnetic fields.

The typical wTF-μSR spectra (i.e. only the oscillatory term $A_iG_x(t)\cos(\omega t+\theta_i)$] of Eq. (1) normalized to the calibration value for A_i) are shown in Fig. 8 for backward counter, $T=150$ K and $H=100$ and 5.3 Oe.

On the spectrum for $H=100$ Oe we observe only about 60% of muons, the diamagnetic fraction which experience the external magnetic field.

For $H=5.3$ Oe the same fraction precess with the much smaller frequency 72 kHz (63%, hardly visible on this time scale), but on the top of it we could distinguish two other components.

About 5% of amplitude oscillates with the frequency $f=7.9$ MHz characteristic for the muonium i.e. the bound state of positive muon and electron. For such state the standard electronics used in our experiments is able to register only the half of the muonium signal oscillating with the frequency of about 100 times the μ^+ precession (given roughly by the gyromagnetic factor of an electron in the pair). The another half of the amplitude is oscillating with even higher frequency (given in this field range mainly by the strong hyperfine coupling between the bound electron and muon—for ZnS 3547.8 MHz [23]). Such frequency is beyond our time resolution (in GHz range). Hence we can state that about 10% of muons stopped in the nonmagnetic parts of the ZnS:Cu crystal form the muonium complexes.

Another 27% of the signal is strongly damped (with the damping parameter $\sigma=155\pm18\ \mu s^{-1}$), what could be observed for first 0.02 μs. There might be two interpretations of that part. The first one associates that signal with the muons stopped in the magnetic parts of the sample, where strong internal magnetic fields (of the order of 10 kOe at the muon site) randomly add to the external field.

The another interpretation may connect that signal to so called "delayed electron capture ($Mu^\circ \rightarrow Mu^-$)" reported for pure ZnS crystals [24]. In ZnS the muonium is believed to be a deep acceptor center, thus the diamagnetic μSR signal being given by the Mu^- center (interstitial μ^+ binding 2 electrons). The capture of the second electron leads at low temperatures to rapid muon spin depolarization seen in wTF-μSR spectra as so called "missing fraction". The fractions of diamagnetic, Mu° and missing signal at 10 K were reported in Ref. [23] to be respectively 20(1)%, 19(3)% and 61(3)% and in Ref. [24]—about 20%, 30% and 50%. In the intermediate temperatures (between 50 and 250 K) the delayed electron capture in pure ZnS caused strong increase of the diamagnetic signal and disappearance of muonium signal. In our case the amplitude of diamagnetic signal does not change significantly with temperature. For $H=100$ Oe and temperatures of 5.3, 9, 52 and 150 K the diamagnetic fraction was $60.2\pm0.3\%$, $60.8\pm0.4\%$, $61.2\pm0.3\%$ and $60.1\pm0.3\%$, respectively. Most probably in our ZnS:Cu crystals the life time of the carriers excited by stopping muon is so short that most of the muons do not capture electron and the diamagnetic signal is due to Mu^+ center.

Thus we may conclude that the first interpretation of the fast relaxing signal is much more plausible and for $T=150$ K the $27\pm1\%$ of the sample volume fraction exhibits strong magnetism, whereas the rest is nonmagnetic where the signals due to Mu^+ and Mu° centers are observed.

A $T=300$ K and $H=5.3$ Oe the fractions were $25\pm2\%$ magnetic, $62.1\pm0.6\%$ of nonmagnetic μ^+ and $6.5\pm0.7\%$ of Mu° signal, what corresponds to the 13% of muonium fraction.

Our experiments suggest that these volume fractions do not change significantly with temperature. The volume fraction of the magnetic phase strongly suggests, that the observed magnetism is not induced by impurities but is an intrinsic behavior.

The low intensity of XRD peaks (near 30°) point to a few percent of ZnO in the sample volume. The uSR data obtained at room temperature indicate that 25% of the volume of the sample is magnetic signifying that observed bulk magnetism is coming from Cu doped ZnS.

4. Conclusions

The results presented in this paper can be interpreted in the framework of the model developed by Dietl [8,9,18]. According to this model magnetism in ZnS doped with copper is highly nonuniform due to nonrandom distribution of magnetic impurities in the sample. The sample is decomposed into nanoregions with low and high concentration of magnetic ions. The volume and shape of the nanoregions together with their magnetic anisotropy determine blocking temperature of the system. Above this temperature the behavior of the system is typical of superparamagnets. A broad structural characterization of the samples and a detailed investigation of their transport properties would be required for better understanding of the physics of the complex system studied in the present work.

Acknowledgments

The μSR experiments were performed at the Swiss Muon Source, Paul Scherrer Institute, Villigen, Switzerland. The authors are grateful to Prof. W. Paszkowicz for assistance in X-ray diffraction measurements. CB acknowledges support by the Schweizer Nationalfonds (SNF) in Grant 200020-119784 and AG–partial support by the MTKD-CT-2005-029671 project from the EU.

References

[1] T. Jungwirth, K.Y. Wang, J. Masek, K.W. Edmonds, J. Konig, J. Sinova., M. Polini, N.A. Goncharuk, A.H. MacDonald, M. Sawicki, A.W. Rushforth, R.P. Campionm, L.X. Zhao, C.T. Foxon, B.L. Gallagher, Phys. Rev. B 72 (2005) 165204.
[2] M.L. Reed, N.A. El-Masry, H.H. Stadelmaier, M.K. Ritums, M.J. Reed, C.A. Parker, J.C. Roberts, S.M. Bedair, Appl. Phys. Lett. 79 (2001) 3473.
[3] G.T. Thaler, M.E. Overberg, B. Gila, R. Frazier, C.R. Abernathy, S.J. Pearton, J.S. Lee, S.Y. Lee, Y.D. Park, Z.G. Zhim, Appl. Phys. Lett. 80 (2002) 3964.
[4] N. Theodoropoulou, G.P. Berera, V. Misra, P. LeClair, J. Phillip, J.S. Moodera, Phys. Rev. Lett. 89 (2002) 107203.
[5] P. Sharma, A. Gupta, K.V. Rao, F.J. Owens, R. Sharma, R. Ahuja, J.M. Osorio Guillen, B. Johansson, G.A. Gehring, Nat. Mater. 2 (2003) 673;
P. Sharma, A. Gupta, F.J. Owens, A. Inoue, K.V. Rao, J. Magn. Magn. Mater. 282 (2004) 115.
[6] A. Gupta, F.J. Owens, K.V. Rao, Z. Iqbal, J.M. Osorio Guillen, R. Ahuja, Phys. Rev. B 74 (2006) 224449.
[7] T. Dietl, H. Ohno, F. Matsurkura, J. Gilbert, D. Ferrand, Science 287 (2000) 1019.
[8] T. Dietl, Nat. Mater. 5 (2006) 673.
[9] T. Dietl, Acta Phys. Pol. A 111 (2007) 27.
[10] Z. Chang-wen, Y. Shi-shen, J. Appl. Phys. 107 (2010) 043913.
[11] Y. Huiyu, L. Yuqi, G. Yanrui, S. Qinggong, C. Yifei, Physica B 406 (2011) 545.
[12] P. Dutta, M.S. Seehra, Y. Zhang, I. Wender, J. Appl. Phys. 103 (2008) 07D104.
[13] J.R. Neal, A.J. Behan, R.M. Ibrahim, H.J. Blythe, M. Ziese, A.M. Fox, G.A. Gehring, Phys. Rev. Lett. 96 (2006) 197208.
[14] W.Q. Peng, G.W. Cong, S.C. Qu, Z.G. Wang, Opt. Mater. 29 (2006) 313.
[15] O. Brafman, S.S. Mitra, Phys. Rev. 171 (1968) 931.
[16] J. Serrano, A.H. Romero, F.J. Manjón, R. Lauck, M. Cardona, A. Rubio, Phys. Rev. B 69 (2004) 014301.
[17] F.J. Owens, J. Phys. Chem. Solids 66 (2005) 793.
[18] T. Dietl, J. Appl. Phys. 103 (2008) 07D111.
[19] M.D. Sastry, K.S. Ajayakumar, R.M. Kadam, G.M. Phatak, R.M. Iyer, Physica C 170 (1990) 41.
[20] F.J. Owens, Physica C 353 (2001) 265.
[21] H. Montiel, G. Alvarez, I. Betancourt, R. Zamorano, R. Valenzuela, Appl. Phys. Lett. 86 (2005) 072503.
[22] M. Golosovsky, P. Monod, P.K. Muduli, R.C. Budhani, L. Mechin, P. Perna, Phys. Rev. B 76 (2007) 184414.
[23] B.D. Patterson, Rev. Mod. Phys. 60 (1988) 69.
[24] R.C. Vilão, J.M. Gil, A. Weidinger, H.V. Alberto, J. Piroto Duarte, N. Ayres de Campos, R.L. Lichti, K.H. Chow, S.P. Cottrell, S.F.J. Cox, Phys. Rev. B 77 (2008) 235212.